Does antikaon condensed phase exist in neutron stars?

K. Miyazaki

Abstract

Neutron star matter including all the baryon octets and condensed antikaons is investigated by the extended Zimanyi-Moszkowski model. It is only the relativistic mean-field model to take into account both the (hidden) strange mesons and the effectively density-dependent meson-baryon coupling constants. Even if we assume the deep $\bar{K}$ optical potential $U_{\bar{K}} = -160\,\mathrm{MeV}$ and strong $NN\delta$ and $NN\rho$ coupling constants, which are necessary for antikaon condensation in neutron star but are not consistent to the results of the most refined theoretical investigations, the maximum mass of neutron star is lower than the canonical value $1.44M_{\odot}$. Consequently, antikaon condensed phase is unlikely to exist in neutron stars.

Recently there are large interests on kaons in nuclear physics. One of them is the possibility that the antikaon condensed phase [1] may be formed in dense strange baryonic medium as neutron star (NS) matter because the antikaons feel an attraction in the medium. For one thing the existence of such a novel phase depends on the strength of the attraction, and for another the realistic description of the dense medium is necessary to predict it reliably. For the former the theoretical investigations [2-7] unfortunately predict the rather wide range of $\bar{K}$ optical potentials being from $U_{\bar{K}} \approx -50\,\mathrm{MeV}$ to $U_{\bar{K}} \approx -180\,\mathrm{MeV}$. For the latter, although the relativistic models are most reliable at present, there are some variants that are essentially different from each other.

The relativistic Brueckner-Hartree-Fock (RBHF) [8] theory is the most fundamental model of nuclear matter, but its extension to include all the baryon octets is not feasible at present. Therefore many studies of NS matter [9] have been done by the relativistic mean-field (RMF) theories based on or inspired by the Walecka model [10]. The most widely used nonlinear extensions [11] of the Walecka model however are not realistic because they do not consider the medium dependences of meson-baryon coupling constants, which are realized in the RBHF theory and are essentially important to dense hadronic matter.

In the RMF models including hyperons, the (hidden) strange mesons σ^* and ϕ [12] should be taken into account for the realistic description of YY interactions. In this respect the so-called DDRH model [13] is not suitable because of the difficulty to include the explicitly density-dependent $YY\sigma^*(\phi)$ coupling constants. Consequently, there remain only two possibilities of the realistic RMF models for dense baryon matter. They are the Zimanyi-Moszkowski (ZM) model [14,15] and the quark-meson coupling (QMC) model [16,17]. In contrast to the DDRH model, these models introduce the density-dependences of the meson-baryon coupling constants implicitly through the effective masses of baryons in the medium.

At present we can find no investigations of the antikaon condensation in NSs by the QMC model including all the baryon octets.[1] On the other hand, the modified ZM model [18-20] was applied to it in Ref. [21] but does not take into account the strange mesons. They are considered by the extended ZM (EZM) model developed in Refs. [22,23]. The purpose of the present work is to investigate the antikaon condensation in NSs by the EZM model.

The EZM model Lagrangian of NS matter composed of baryon octets and leptons is the same as Ref. [23]. We have only to add the contribution of antikaons, which is formally the same as Ref. [24] except that the meson-kaon coupling constants in the present model are renormalized. The resultant energy density becomes

$$\begin{aligned}\mathcal{E} &= \frac{1}{4}\sum_{\substack{B=p,n,\Lambda,\Sigma^+,\\ \Sigma^0,\Sigma^-,\Xi^0,\Xi^-}}\left(3E^*_{BF}\rho_B + M^*_B\rho_{BS}\right) + \frac{1}{4}\sum_{l=e,\mu^-}\left(3E_{lF}\rho_l + m_l\rho_{lS}\right) + \sum_{\bar{K}=\bar{K}^0,K^-} M^*_{\bar{K}}\rho_{\bar{K}} \\ &+ \frac{1}{2}m_\sigma^2\langle\sigma\rangle^2 + \frac{1}{2}m_\omega^2\langle\omega_0\rangle^2 + \frac{1}{2}m_\delta^2\langle\delta_3\rangle^2 + \frac{1}{2}m_\rho^2\langle\rho_{03}\rangle^2 + \frac{1}{2}m_{\sigma^*}^2\langle\sigma^*\rangle^2 + \frac{1}{2}m_\phi^2\langle\phi_0\rangle^2 ,\end{aligned} \tag{1}$$

where ρ_B and ρ_l are the vector densities of the baryons and leptons in NS matter. The ρ_{BS} and ρ_{lS} are their scalar densities. E^*_{BF} and E_{lF} are their Fermi energies. The m_l is mass of each lepton. The $\rho_{\bar{K}}$ is the density of condensed antikaon. The m_σ *etc.* are masses of the mesons and $\langle\sigma\rangle$ *etc.* are their mean-fields.

The effective mass M^*_B of each baryon is

$$M^*_B = M_B - g^*_{BB\sigma}\langle\sigma\rangle - g^*_{BB\delta}\langle\delta_3\rangle I_{3B} - g^*_{BB\sigma^*}\langle\sigma^*\rangle , \tag{2}$$

where M_B is free baryon mass and $I_{3B} = \{1, -1, 0, 1, 0, -1, 1, -1\}$ for $B = \{p, n, \Lambda, \Sigma^+, \Sigma^0, \Sigma^-, \Xi^0, \Xi^-\}$. The renormalized scalar-meson coupling constants $g^*_{BB\sigma}$ *etc.* are found in Ref. [23]. On the other hand, the vector potential V_B is given by

$$V_B = g^*_{BB\omega}\langle\omega_0\rangle + g^*_{BB\rho}\langle\rho_{03}\rangle I_{3B} + g^*_{BB\phi}\langle\phi_0\rangle , \tag{3}$$

where $g^*_{BB\omega}$ *etc.* are the renormalized vector-meson coupling constants [23]. The effective

[1] After we have completed this paper, Ref. [32] has appeared. However it does not take into account the effects of δ meson nor strange mesons. Moreover, its (nonstrange) meson-hyperon coupling constants are not physically realistic. Consequently, Fig. 5(b) in it shows the abundances of Σ hyperons and absence of Ξ hyperons in NS matter. At present, no observation of Σ hypernuclei and the detailed theoretical analyses of Σ^- atomic data and (π^-, K^+) spectra strongly support repulsive Σ-nucleus optical potential. We can therefore expect the absence of Σ hyperons in NS matter. Although we have not shown the particle fractions, there are no Σs in our results because of our physically reasonable choice of the meson-hyperon coupling constants

mass of antikaon is

$$M_{\bar{K}}^{*} = M_K - g_{\bar{K}\bar{K}\sigma}^{*} \langle\sigma\rangle - g_{\bar{K}\bar{K}\delta}^{*} \langle\delta_3\rangle I_{3\bar{K}} - g_{\bar{K}\bar{K}\sigma^*}^{*} \langle\sigma^*\rangle , \tag{4}$$

and its vector potential is

$$V_{\bar{K}} = - g_{\bar{K}\bar{K}\omega}^{*} \langle\omega_0\rangle + g_{\bar{K}\bar{K}\rho}^{*} \langle\rho_{03}\rangle I_{3\bar{K}} - g_{\bar{K}\bar{K}\phi}^{*} \langle\phi_0\rangle , \tag{5}$$

where $M_K = 495.7\,\mathrm{MeV}$ is free kaon mass and $I_{3\bar{K}} = \{1, -1\}$ for $\bar{K} = \{\bar{K}^0, K^-\}$. The vector mean-fields in Eqs. (3) and (5) are given by

$$\langle\omega_0\rangle = \sum_B \frac{g_{BB\omega}^{*}}{m_\omega^2}\rho_B - \sum_{\bar{K}} \frac{g_{\bar{K}\bar{K}\omega}^{*}}{m_\omega^2}\rho_{\bar{K}}, \tag{6}$$

$$\langle\rho_{03}\rangle = \sum_B I_{3B} \frac{g_{BB\rho}^{*}}{m_\rho^2}\rho_B + \sum_{\bar{K}} I_{3\bar{K}} \frac{g_{\bar{K}\bar{K}\rho}^{*}}{m_\rho^2}\rho_{\bar{K}}, \tag{7}$$

$$\langle\phi_0\rangle = \sum_Y \frac{g_{YY\phi}^{*}}{m_\phi^2}\rho_Y - \sum_{\bar{K}} \frac{g_{\bar{K}\bar{K}\phi}^{*}}{m_\phi^2}\rho_{\bar{K}}. \tag{8}$$

Because we treat antikaons as the same footing as baryons [25], the renormalized meson-antikaon coupling constants $g_{\bar{K}\bar{K}\sigma}^{*}$ *etc.* in Eqs. (6)-(8) are derived on the analogy of the renormalized meson-baryon couplings in Refs. [18-23]. They are given by

$$g_{\bar{K}\bar{K}\sigma(\delta,\omega,\rho)}^{*} = \left(1 + \bar{S}_s^{\bar{K}}\right) g_{KK\sigma(\delta,\omega,\rho)} = \left(1 + S_s^{\bar{K}}/M_K\right) g_{KK\sigma(\delta,\omega,\rho)}, \tag{9}$$

$$g_{\bar{K}\bar{K}\sigma^*(\phi)}^{*} = \left(1 + \bar{S}_{\bar{q}}^{\bar{K}}\right) g_{KK\sigma^*(\phi)} = \left(1 + S_{\bar{q}}^{\bar{K}}/M_K\right) g_{KK\sigma^*(\phi)}, \tag{10}$$

where $g_{KK\sigma}$ *etc.* are free meson-kaon coupling constants. The $S_{\bar{q}}^{\bar{K}}$ and $S_s^{\bar{K}}$ are the scalar potential for the constituent $\bar{u}(\bar{d})$ and s quark in antikaons. For $\bar{K}^0$ they are given by

$$\bar{S}_{\bar{d}}^{\bar{K}^0} = \frac{\bar{\sigma}_K^* - 1}{C_{\bar{K}^0}} \left(\bar{\sigma}_K + \bar{\delta}_K\right), \tag{11}$$

$$\bar{S}_s^{\bar{K}^0} = \frac{\bar{\sigma}_K + \bar{\delta}_K - 1}{C_{\bar{K}^0}} \bar{\sigma}_K^*, \tag{12}$$

where

$$C_{\bar{K}^0} = 1 - \left(\bar{\sigma}_K + \bar{\delta}_K\right)\bar{\sigma}_K^*, \tag{13}$$

and we have introduced the reduced mean-fields:

$$\bar{\sigma}_K = \frac{g_{KK\sigma}}{M_K}\langle\sigma\rangle, \quad \bar{\delta}_K = \frac{g_{KK\delta}}{M_K}\langle\delta_3\rangle \quad \text{and} \quad \bar{\sigma}_K^* = \frac{g_{KK\sigma^*}}{M_K}\langle\sigma^*\rangle. \tag{14}$$

The similar expressions for K^- are obtained by changing the signs of $\bar{\delta}_K$ in Eqs. (11)-(13).

As shown in Ref. [23], the scalar mean-fields $\langle\sigma\rangle$, $\langle\delta_3\rangle$ and $\langle\sigma^*\rangle$ are expressed by the effective masses of proton $m_p^* = M_p^*/M_N$, neutron $m_n^* = M_n^*/M_N$ and lambda $m_\Lambda^* = M_\Lambda^*/M_\Lambda$, and so the effective masses and the coupling constants of other baryons are also expressed by them. The effective masses of antikaons are given by

$$m^*_{\bar{K}^0(K^-)} = \frac{M^*_{\bar{K}^0(K^-)}}{M_{\bar{K}^0(K^-)}} = \frac{1 - \left(\bar{\sigma}_K \pm \bar{\delta}_K\right) - \bar{\sigma}_K^* + \left(\bar{\sigma}_K \pm \bar{\delta}_K\right)\bar{\sigma}_K^*}{C_{\bar{K}^0(K^-)}}, \tag{15}$$

where $+\bar{\delta}_K$ is for $\bar{K}^0$ and $-\bar{\delta}_K$ is for K^-. The values of m_p^*, m_n^* and m_Λ^* are determined by minimizing the energy density by them. The resultant three equations, whose derivations are tedious but straightforward and so are not shown here, are solved under the β-equilibrium, charge neutral conditions and baryon number conservation [11] in NS matter.

We first take the same meson-baryon coupling constants as the set 4 in Ref. [23]. They are consistent to the most recent information on hyperon interactions from the experimental and theoretical investigations of hypernuclei. Then the meson-kaon coupling constants have to be determined. In this respect we follow Ref. [26]. The same $KK\omega$, $KK\rho$, $KK\sigma^*$ and $KK\phi$ coupling constants are employed. The $KK\sigma$ and $KK\delta$ coupling constants, $g_{KK\sigma} = 2.33$ and $g_{KK\delta} = 7.84$, are determined from KN scattering lengths. The resultant antikaon optical potential in normal nuclear matter at saturation is $U_{\bar{K}} = -160.5\,\mathrm{MeV}$. The value nearly agrees with the phenomenological analysis [5] from K^- atomic data.

The results using the obtained coupling constants are shown by the dashed curves in figures. Figure 1 shows the chemical potential of $\bar{K}^0$ and the difference between the chemical potentials of K^- and electron. Antikaon condensations are only possible if the curves cross zeros. Figures 2 and 3 show the equations of state (EOSs) and the mass sequences of cold non-rotating NSs. It is seen in Fig. 1 that the K^- condensation appears above the total baryon density $\rho = 0.373\,\mathrm{fm}^{-3}$ while we cannot find the $\bar{K}^0$ condensation. The resultant EOS in Fig. 2 however becomes unphysical at high densities. Therefore the mass sequence of NSs is not calculated.

As was pointed out in Ref. [26], the δ-meson contribution is crucial to reproduce KN scattering lengths. The above unphysical EOS therefore may be due to the weak $NN\delta$ and $NN\rho$ coupling constants, $\left(g_{NN\delta}/m_\delta\right)^2 = 0.39\,\mathrm{fm}^2$ and $\left(g_{NN\rho}/m_\rho\right)^2 = 0.82\,\mathrm{fm}^2$ from Bonn A potential in Ref. [8]. The $\bar{K}$ condensation largely depletes the pressure of NS matter because its contribution weakens $\langle\omega_0\rangle$ and $\langle\phi_0\rangle$ mean-fields as seen in Eqs. (6) and (8). On the other hand, the ρ mean-field $\langle\rho_{03}\rangle$ in NS matter always has negative value because of the predominance of neutron over proton at lower densities and the abundance of K^- at higher densities. Therefore the strong $NN\rho$ coupling constant enlarges the absolute value of ρ mean-field and relieves the depletion of pressure by K^- condensation.

However we cannot increase $NN\rho$ coupling alone because both the $NN\delta$ and $NN\rho$ couplings are strongly correlated [27]. Then we use the same $NN\delta$ coupling constant as Ref. [26] and determine $NN\rho$ coupling constant so as to reproduce the symmetry-energy of nuclear matter being 28 MeV [28]. The results using these strong $NN\delta$ and $NN\rho$ couplings, $(g_{NN\delta}/m_\delta)^2 = 1.43\,\mathrm{fm}^2$ and $(g_{NN\rho}/m_\rho)^2 = 1.89\,\mathrm{fm}^2$, are shown by the solid curves in the figures. (In this case the $KK\delta$ coupling constant becomes $g_{KK\delta} = 7.13$, which is somewhat larger than the value in Ref. [26].) As seen in Fig. 1, the K^- condensation appears above the baryon density $\rho = 0.353\,\mathrm{fm}^{-3}$ while the $\bar{K}^0$ condensation never appears. We stopped the calculation when the effective mass of neutron becomes negative at $\rho = 0.772\,\mathrm{fm}^{-3}$ because of the strong $NN\delta$ coupling. The abundance of K^- largely delays the appearances of hyperons and so there is only Λ hyperon above $\rho = 0.530\,\mathrm{fm}^{-3}$. The K^- condensation causes the first-order phase transition into the EOS in Fig. 2. We employ the Maxwell construction to determine the equilibrium state or the mixed phase of the two phases, the pure baryon and the K^- condensed phases. By integrating the TOV equation [29], the resultant mass sequence of NSs in Fig. 3 predicts the maximum mass $1.28M_\odot$ being lower than the canonical value $1.44M_\odot$ [30]. This casts a doubt on the existence of $\bar{K}$ condensed phase in NSs. Even if the Gibbs construction [25] of the mixed phase is employed, the result would not be altered largely.

Next, we calculate the NS matter again by determining the $KK\sigma$ coupling constant $g_{KK\sigma} = 1.78$ phenomenologically [25] to reproduce somewhat shallower $\bar{K}$ optical potential $U_{\bar{K}} = -140\,\mathrm{MeV}$ than $U_{\bar{K}} \simeq -160\,\mathrm{MeV}$ obtained above. The dashed-dotted and dotted curves in the figures are the results using the strong and weak $NN\delta$ and $NN\rho$ coupling constants respectively. As seen in Fig. 1, there are no antikaons in NSs and so the dotted curve is equivalent to the result by the set 4 in Ref. [23]. Now, it has been confirmed that the antikaon appears only if its optical potential in the saturated nuclear matter is deeper than $U_{\bar{K}} = -160\,\mathrm{MeV}$. However the deep potential $U_{\bar{K}} \simeq -160\,\mathrm{MeV}$ obtained by the simple one-boson-exchange model [26] is not consistent to the recent refined coupled-channel calculations [6,7], which predict much shallower potentials, and so cannot be regarded as a physically reasonable value.

Although the EOS of the dotted-dashed curve in Fig. 2 is stopped at $\rho = 0.733\,\mathrm{fm}^{-3}$ where the neutron effective mass becomes negative, there are only small differences between the dotted and dashed-dotted curves in the figures. The maximum masses of NS in Fig. 3 are $1.615M_\odot$ and $1.598M_\odot$ respectively. We can therefore see that the EZM model without $\bar{K}$ condensations is stable against the large differences of isovector-meson coupling constants. On the contrary, the antikaon condensed phase is unstable as was seen in the difference between EOSs of the solid and dashed curves. This also suspects the existence of $\bar{K}$ condensations in NSs.

The above results indicate that antikaon condensed phase is unlikely to exist in NSs. The similar conclusion has been recently derived [31] from a different point of view. Moreover, we have to stress that the strong $NN\delta$ and $NN\rho$ coupling constants used for the solid curves in the figures are never justified. The study of Ref. [8] has revealed that the NN scattering analysis is not sensitive to $NN\delta$ coupling but the RBHF calculation of nuclear matter saturation obviously excludes the strong $NN\delta$ coupling. For a definite symmetry-energy of nuclear matter, the strong $NN\delta$ coupling requires strong $NN\rho$ coupling [27], which however is not consistent to Bonn A potential in Ref. [8]. Almost calculations by the nonlinear Walecka model have not taken into account δ meson but assumed strong $NN\rho$ couplings. If the δ meson is introduced, their $NN\rho$ couplings become much stronger and so unphysical. Usually, this shortcoming is excused by mentioning that the meson-baryon coupling constants in the models are the effective ones. Fortunately or not, such a cheating is not applicable to the EZM model in which the effective renormalized coupling constants are determined self-consistently in the medium. We therefore have to specify the free coupling constants obtained from NN scattering data but not the effective ones.

The NS matter including all the baryon octets and condensed antikaons is investigated by the extended Zimanyi-Moszkowski model. It is only the RMF model to take into account both the (hidden) strange mesons mediated between hyperons and the effectively density-dependent meson-baryon and antikaon coupling constants. If we assume the $\bar{K}$ optical potential $U_{\bar{K}} = -140\,\mathrm{MeV}$ that is still much deeper than the values obtained by recent theoretical investigations, there are no antikaons in NS matter. If the $KK\sigma$ coupling constant is determined from KN scattering length, slightly deeper $\bar{K}$ optical potential $U_{\bar{K}} = -160\mathrm{MeV}$ is obtained and so the K^- appears. However, using the relatively weak coupling constants of isovector mesons from Bonn A NN potential, the resultant EOS becomes unphysical. Even if the much stronger coupling constants are used, the maximum mass of NS is lower than the canonical value $1.44M_{\odot}$. Consequently, we conclude that antikaon condensation is unlikely to occur in NSs regardless of the uncertainties of meson-antikaon coupling constants.

References

[1] R. Knorren, M. Prakash and P.J. Ellis, Phys. Rev. **C52** (1995) 3470, [arXiv:nucl-th/9506016].

[2] V. Koch, Phys. Lett. **B337** (1994) 7.

[3] T. Waas and W. Weise, Nucl. Phys. **A625** (1997) 287.

[4] A. Ramos and E. Oset, arXiv:nucl-th/9810014.

[5] E. Friedman, A. Gal, J. Mareš and A. Cieplý, Phys. Rev. **C60** (1999) 024314, [arXiv:nucl-th/9804072].

[6] A. Ramos and E. Oset, Nucl. Phys. **A671** (2000) 481.

[7] A. Cieplý, E. Friedman, A. Gal and J. Mareš, Nucl. Phys. **A696** (2001) 173,

[8] R. Brockmann and R. Machleidt, Phys. Rev. **C42** (1990) 1965.

[9] J.M. Lattimer and M. Prakash, Astrophys. J. **550** (2001) 426.

[10] B.D. Serot and J.D. Walecka, *Advances in Nuclear Physics*, Vol. **16** (Plenum, New York, 1986).

[11] S. Pal, D. Bandyopadhyay and W. Greiner, Nucl. Phys. **A674** (2000) 553, [arXiv:astro-ph/0001039].

[12] J. Schaffner, C.B. Dover, A. Gal, C. Greiner and H. Stőker, Phys. Rev. Lett. **71** (1993) 1328.

[13] S. Banik and D. Bandyopadhyay, Phys. Rev. **C66** (2002) 065801, [arXiv:astro-ph/0205532].

[14] J. Zimanyi and S.A. Moszkowski, Phys. Rev. **C42** (1990) 1416.

[15] I. Bednarek, M. Keska and R. Manka, Phys. Rev. **C68** (2003) 035805, [arXiv:nucl-th/0212065].

[16] K. Tsushima, K. Saito, A.W. Thomas and S.V. Wright, Phys. Lett. **B429** (1998) 239, [arXiv:nucl-th/9712044].

[17] S. Pal, M. Hanauske, I. Zakout, H. Stőker and W. Greiner, Phys. Rev. **C60** (1999) 015802, [arXiv:nucl-th/9905010].

[18] K. Miyazaki, CERN Document Server (CDS) ext-2003-062 revised by Mathematical Physics Preprint Archive (mp_arc) 05-178.

[19] K. Miyazaki, CERN Document Server (CDS) ext-2003-077 revised by Mathematical Physics Preprint Archive (mp_arc) 05-190.

[20] K. Miyazaki, CERN Document Server (CDS) ext-2004-010 revised by Mathematical Physics Preprint Archive (mp_arc) 05-199.

[21] K. Miyazaki, CERN Document Server (CDS) ext-2004-036 revised by Mathematical Physics Preprint Archive (mp_arc) 05-206.

[22] K. Miyazaki, CERN Document Server (CDS) ext-2004-071 revised by Mathematical Physics Preprint Archive (mp_arc) 05-216.

[23] K. Miyazaki, CERN Document Server (CDS) ext-2004-134 revised by Mathematical Physics Preprint Archive (mp_arc) 05-224.

[24] S. Banik and D. Bandyopadhyay, Phys. Rev. **C64** (2001) 055805, [arXiv:astro-ph/0106406].

[25] N.K. Glendenning and J. Schaffner, Phys, Rev. **C60** (1999) 025803, [arXiv:astro-ph/9810290].

[26] J. Schaffner and I.N. Mishustin, Phys. Rev. **C53** (1996) 1416, [arXiv:nucl-th/9506011]; J. Schaffner, I.N. Mishustin and J. Bondorf, Nucl. Phys. **A625** (1997) 325.

[27] S. Kubis and M. Kutschera, Phys. Lett. **B399** (1997) 191, [arXiv:astro-ph/9703049].

[28] J.M. Pearson and R.C. Nayak, Nucl. Phys. **A668** (2000) 163.

[29] W.D. Arnett and R.L. Bowers, Astrophys. J. Suppl. **33** (1977) 415.

[30] J.M. Weisberg and J.H. Taylor, Proceedings of August 2002 meeting "Radio Pulsars" in Chania, Crete, ASP Conference Series Vol. CS-302 (2003), M. Bailes, D.J. Nice and S.E. Thorsett, eds. [arXiv:astro-ph/0211217].

[31] Th. Roth, M. Buballa and J. Wambach, arXiv:nucl-th/0504056.

[32] D.P. Menezes, P.K. Panda and C. Providência, arXiv:astro-ph/0506196.

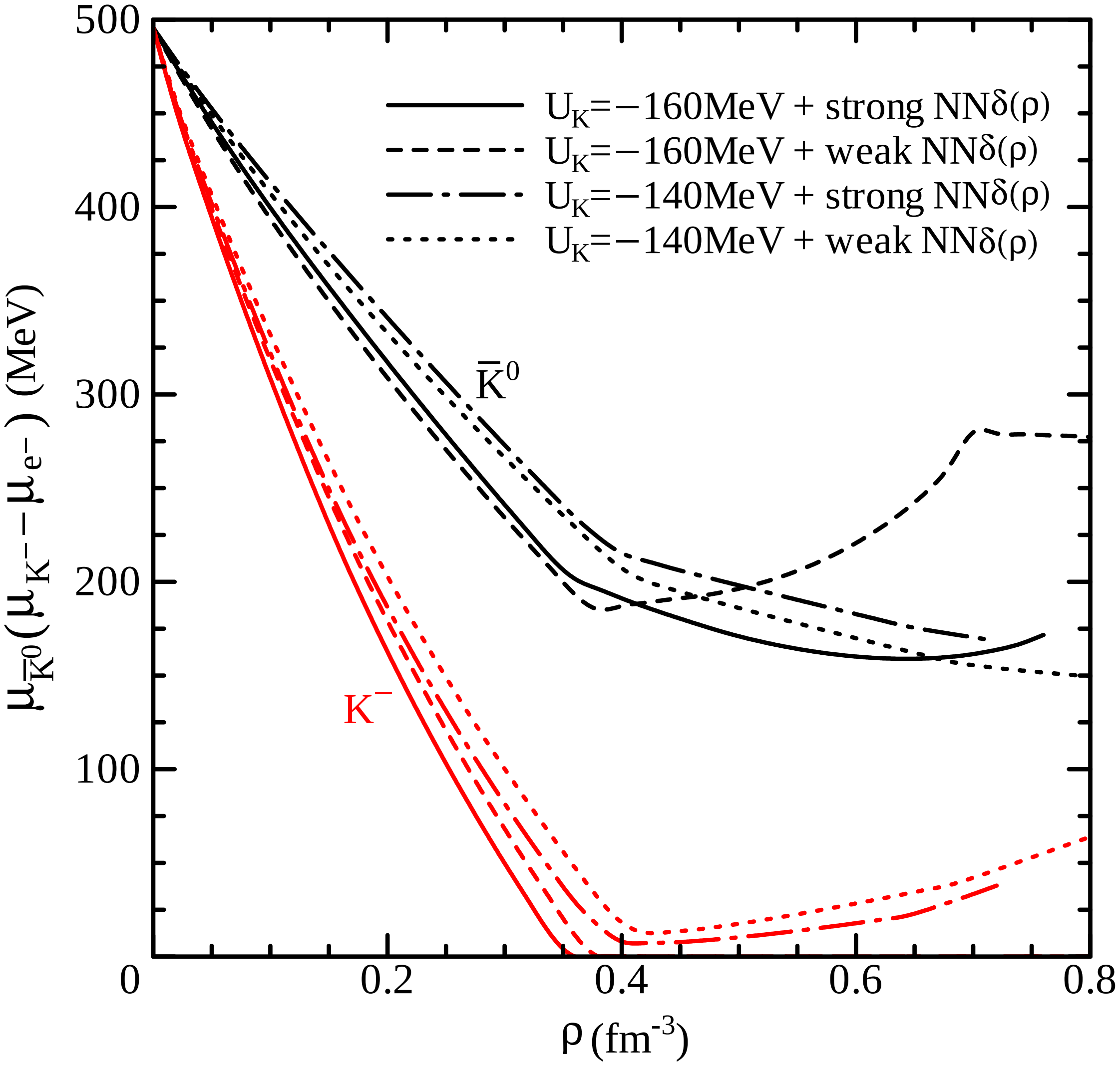

Figure 1: The chemical potential of $\bar{K}^0$ (black curves) and the difference between the chemical potentials of K^- and electron (red curves) as functions of the total baryon density. The solid and dashed curves are the results using the $\bar{K}$ optical potential in saturated nuclear matter of $U_{\bar{K}} = -160\,\mathrm{MeV}$. The former assumes the strong $NN\delta$ and $NN\rho$ coupling constants, $(g_{NN\delta}/m_\delta)^2 = 1.43\,\mathrm{fm}^2$ and $\left(g_{NN\rho}/m_\rho\right)^2 = 1.89\,\mathrm{fm}^2$ from Ref. [26] while the latter assumes the weak ones, $(g_{NN\delta}/m_\delta)^2 = 0.39\,\mathrm{fm}^2$ and $\left(g_{NN\rho}/m_\rho\right)^2 = 0.82\,\mathrm{fm}^2$ from Ref. [8]. The dashed-dotted and dotted curves are the results using $U_{\bar{K}} = -140\,\mathrm{MeV}$ with the strong and weak $NN\delta$ and $NN\rho$ couplings respectively.

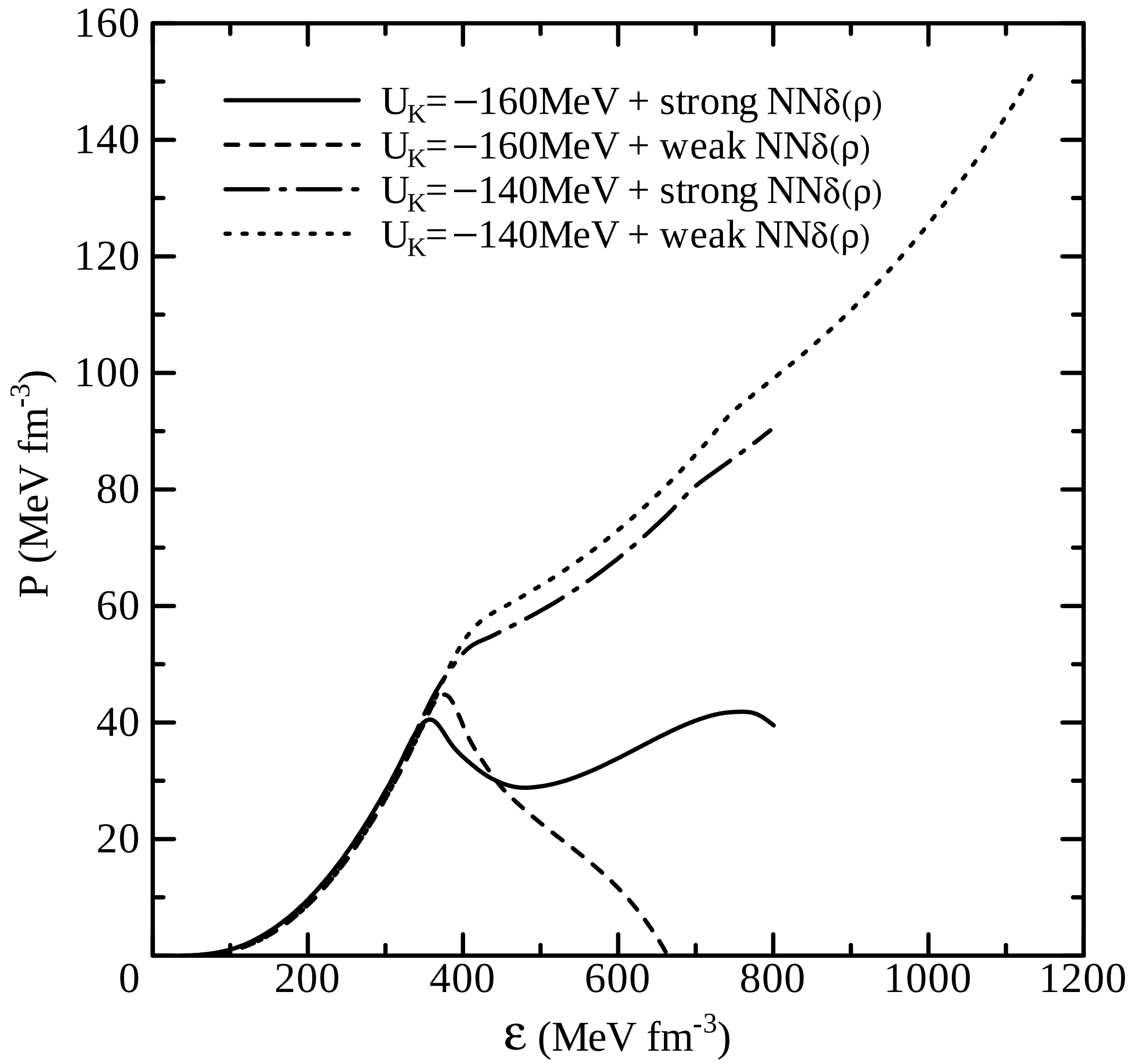

Figure 2: The EOSs of cold non-rotating NSs. The curves are the same as Fig. 1.

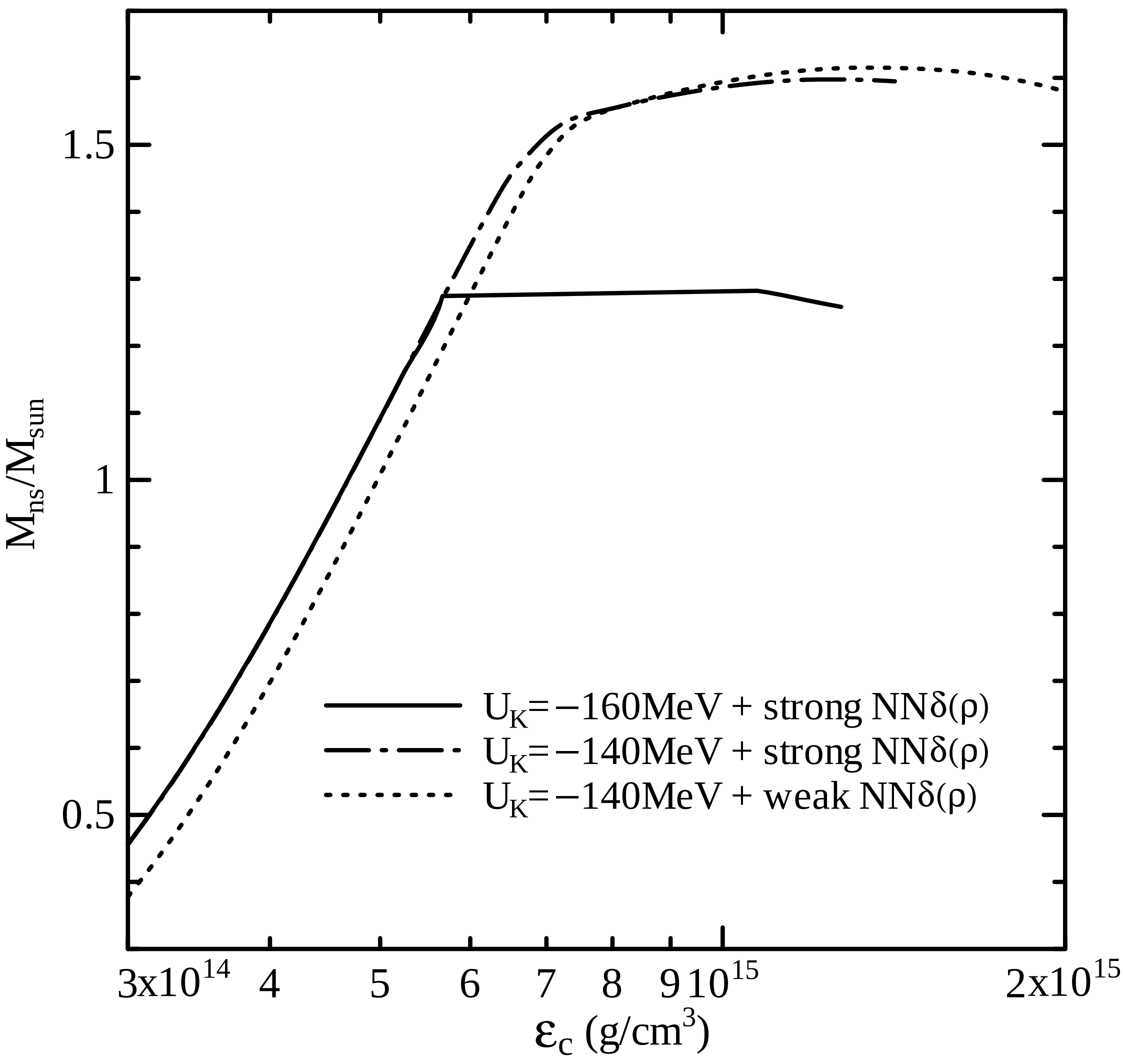

Figure 3: The mass sequences of cold non-rotating NSs by using the EOSs in Fig. 2.